

Quench-induced breathing mode of one-dimensional Bose gases

Bess Fang, Giuseppe Carleo, and Isabelle Bouchoule
*Laboratoire Charles Fabry, Institut d'Optique, Univ Paris Sud 11,
2 avenue Augustin Fresnel, F-91127 Palaiseau cedex, France*
(Dated: July 16, 2018)

We measure the position- and momentum-space breathing dynamics of trapped one-dimensional Bose gases at finite temperature. The profile in real space reveals sinusoidal width oscillations whose frequency varies continuously through the quasicondensate to ideal Bose gas crossover. A comparison with theoretical models taking temperature into account is provided. In momentum space, we report the first observation of a frequency doubling in the quasicondensate regime, corresponding to a self-reflection mechanism due to the repulsive interactions. Its disappearance through the crossover is mapped out experimentally, giving insights to the dynamics of the breathing evolution.

PACS numbers: 03.75.Kk, 67.85.-d

The field of ultracold atomic and molecular gases has gained increasing significance in the study of nonequilibrium phenomena in quantum many-body systems. The accurate time-dependent control of microscopic parameters enables the realization of prototypical nonequilibrium processes, complementary to those studied in condensed matter physics. In particular, isolated quantum many-body systems can be driven out of equilibrium and accurately monitored. The realization of such experimental simulators [1] therefore constitutes a unique tool to investigate fundamental questions. Remarkable examples are the observation of a light-cone effect in the spreading of correlations [2, 3], as well as the studies of quantum ergodicity [1, 4–6], where prethermalisation was observed in (nearly) integrable systems.

One-dimensional (1D) systems are ideal test benches for the study of out-of-equilibrium phenomena because of their intrinsic strong correlations and the possibility to realize integrable models. The experimental investigation of their quantum dynamics is of particular relevance in clarifying questions for which a theoretical treatment is challenging. The understanding of the time-dependent behavior of interacting quantum systems is indeed restricted to a few limiting cases [7], and plagued by the lack of systematic *ab initio* approaches. This stands in contrast to the well consolidated understanding of thermodynamic properties of such systems, for which exact analytical and numerical results are available [8].

Among the simplest out-of-equilibrium situation is the dynamics of a gas after a sudden change (quench) of the external harmonic potential in which the atoms are confined. The resulting coherent, breathing-like oscillations of the atomic cloud are governed by the collective excitations of the quantum gas, and serve to identify the quasicondensate (qBEC) regime [9] and strongly correlated phases in 1D [10]. The sum-rule approach has had a remarkable success in the prediction of the breathing frequencies at zero temperature [11, 12]. Nonetheless, numerous fundamental questions remain open. These questions concern the general mechanism of mass transport

in interacting quantum systems as well as its counterpart in momentum space. In particular, the effect of temperature on both the lifetime and the frequency of the collective mode cannot be accessed in terms of the standard sum-rule approach. Moreover, breathing oscillations of the momentum distribution provide complementary insight on the dynamics of interacting quantum gases, information which is not yet investigated experimentally nor accessible theoretically to date.

In this Letter, we study experimentally the breathing mode of harmonically confined 1D Bose gases at finite temperature, comparing the evolution in real and momentum space. We report the first observation of a self-reflection mechanism due to repulsive interaction, expected of a strongly interacting system [13]. We measure how the dynamics evolves through the qBEC to ideal Bose gas (IBG) crossover, and develop two complementary theoretical treatments for the breathing modes, taking finite-temperature effects into account. The combination of an exact short-time expansion of the dynamics and a long-wavelength hydrodynamic analysis reveals that the finite-temperature mass transport happens in an isentropic way, and provides a qualitatively good agreement with the experimental observations.

System and quench protocol. The Lieb-Liniger (LL) model of 1D bosons in continuum, with a Hamiltonian $H_{\text{LL}} = \sum_j \frac{p_j^2}{2m} + \sum_{j < k} g_{1\text{D}} \delta(z_j - z_k)$, where m is the particle mass, and $g_{1\text{D}} (> 0)$ is the coupling constant, is realized experimentally for gases confined in elongated traps, provided the transverse degrees of freedom are frozen out [14]. Various experimental probes have been developed for such gases, permitting not only thermometry methods [15–20], but also the study of nonequilibrium behavior. Of special importance is the measurement of the momentum distribution, now feasible via Bragg spectroscopy [21] or focusing technique [20].

Our experiment prepares a single tube of ^{87}Rb gas using an atom-chip setup [17]. The final samples typically constitute 800 to 8000 atoms for this experiment. The *in situ* density profile [15] indicates a temperature around

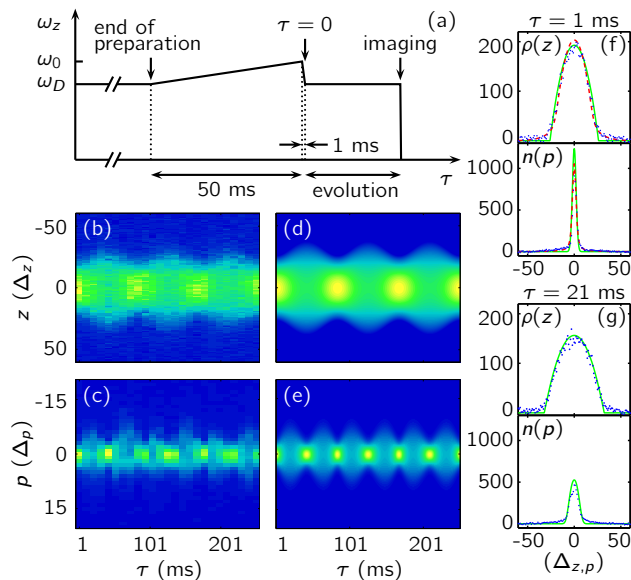


FIG. 1. (Color online) Quench sequence and subsequent density evolution in position and momentum space for a qBEC (data A). (a) Longitudinal trapping frequency ω_z as a function of time τ . (b) $\rho(z, \tau)$, (c) $n(p, \tau)$, experimental data (in atoms/pixel). (d), (e), corresponding plots from *ab initio* scaling calculation. (f) and (g) show instantaneous $\rho(z)$, $n(p)$ at $\tau = 1$ and 21 ms. Experimental data (dots) are compared with the scaling solutions (solid lines). QMC calculation of $n(p, \tau)$ (dashed line) is shown in (f). z (p) is in units of pixels Δ_z (Δ_p), with $\Delta_z = 2.7 \mu\text{m}$, and $\Delta_p = 0.14 \hbar/\mu\text{m}$.

100 nK, corresponding to a central chemical potential $\mu_0 \in [0.04, 0.5] \times k_B T$ [35]. Since the transverse confinement $\omega_\perp = 2\pi \times 2$ kHz, we have $\mu_0 \ll k_B T \simeq \hbar\omega_\perp$, achieving a nearly 1D scenario. The breathing mode is excited by quenching the axial confinement ω_z from ω_0 to ω_D , see Fig. 1(a) for a sketch. We keep the quench strength $\alpha \equiv \omega_0/\omega_D \simeq 1.3$ constant. The resulting cloud evolves for a duration τ before an absorption image is taken, either *in situ* to yield the density profile $\rho(z, \tau)$, or at focus to yield the momentum distribution $n(p, \tau)$. By varying τ , we map out the evolution in real and momentum space.

Quasicondensate regime. We start by considering the qBEC regime: Figures 1(b) and (c) show $\rho(z, \tau)$ and $n(p, \tau)$ for a data set that lies in this regime (data A). The time evolution of these two quantities reveals a remarkable frequency mismatch. In order to elucidate its origin, we use the hydrodynamic equations (HDE) [36]

$$\begin{aligned} \partial_\tau \rho + \partial_z(\rho v) &= 0, \\ \partial_\tau v + v \partial_z v &= -\partial_z \left(\frac{1}{2} \omega_D^2 z^2 \right) - \frac{1}{m\rho} \partial_z P, \end{aligned} \quad (1)$$

where $\rho = \rho(z, \tau)$ and $v = v(z, \tau)$ are the density and velocity fields, and P is the pressure. For a qBEC, $P = g_{1D} \rho^2/2$, so that the scaling solution $\rho(z, \tau) = \frac{1}{b(\tau)} \rho_0\left(\frac{z}{b(\tau)}\right)$ [23] is valid provided ρ_0 is the steady state inverted parabola, and the scaling factor b obeys $\ddot{b} +$

$\omega_z(\tau)^2 b = \frac{\omega_0^2}{b^2}$. Such $\rho(z, \tau)$ is periodic in time with a frequency $\omega_{Bz} \simeq \sqrt{3}\omega_D$. Neglecting thermal fluctuations, it follows that the momentum distribution satisfies [23] $n(p, \tau) \propto \rho_0\left(\frac{bp}{bm}\right)$, which is periodic in time with a frequency $\omega_{Bp} = 2\omega_{Bz}$. Minimal momentum width occurs when the real-space distribution is both the largest and the thinnest. The latter scenario, which does not occur for a non-interacting gas, corresponds to a self-reflection of the cloud due to repulsive interactions. The frequency doubling ($\omega_{Bp} = 2\omega_{Bz}$) is thus a direct consequence of atomic interactions. In higher dimensions, the scaling solutions also predicts a frequency doubling of the breathing modes [37]. What may have prevented its observation is perhaps the fact that early experiments using time-of-flight (TOF) techniques do not measure the true momentum distribution due to the contribution of interaction energy.

It is worth mentioning that such a momentum-space frequency doubling in the oscillatory behavior of w_p , the half width at half maximum (HWHM) in momentum space, is expected to occur for a Tonks gas ($g_{1D} \rightarrow +\infty$) [25]: the momentum distribution for large α oscillates between a Fermi-like and a Bose-like distribution, a thin Bose-like distribution occurring both when the cloud is the thinnest and the largest [13], while in the expansion and compression phases the momentum distribution is dominated by the large Fermi-like hydrodynamic component. This marks the difference between the breathing behaviour of a strongly interacting 1D Bose gas and that of a noninteracting gas, even though the breathing frequency in real space is $\omega_{Bz} = 2\omega_D$ for both cases. Similar collective oscillations of strongly interacting 1D Bose gases have been studied in two experiments [4, 10] to our knowledge, neither reporting any frequency doubling. In the former [4], a different excitation scheme is employed, potentially rendering the frequency doubling inaccessible. In the latter [10], the finite TOF may have prevented the direct measurement of the momentum distribution.

In our experiment the momentum-space frequency doubling is clearly seen in Fig. 1(b-c). Moreover, the data are in good agreement with the zero-temperature theory above, whose predicted real- and momentum-space density evolutions for a system initially at equilibrium in the trap of frequency ω_0 are shown in Fig. 1(d-e), with $n(p, \tau)$ broadened to account for finite resolution [38]. For a more quantitative comparison, we show two frames of the instantaneous densities. At $\tau = 1$ ms (minimal *in situ* width, Fig. 1(f)), the scaling solution predicts a vanishing momentum width, but thermal fluctuations dominate such that the finite-temperature momentum distribution computed using quantum Monte Carlo (QMC) methods [20] (dashed lines) accounts for the data better than the sole effect of resolution [39]. However, thermal fluctuations are small corrections at $\tau = 21$ ms (maximal momentum width, Fig. 1(g)), and both $\rho(z)$ and $n(p)$ are

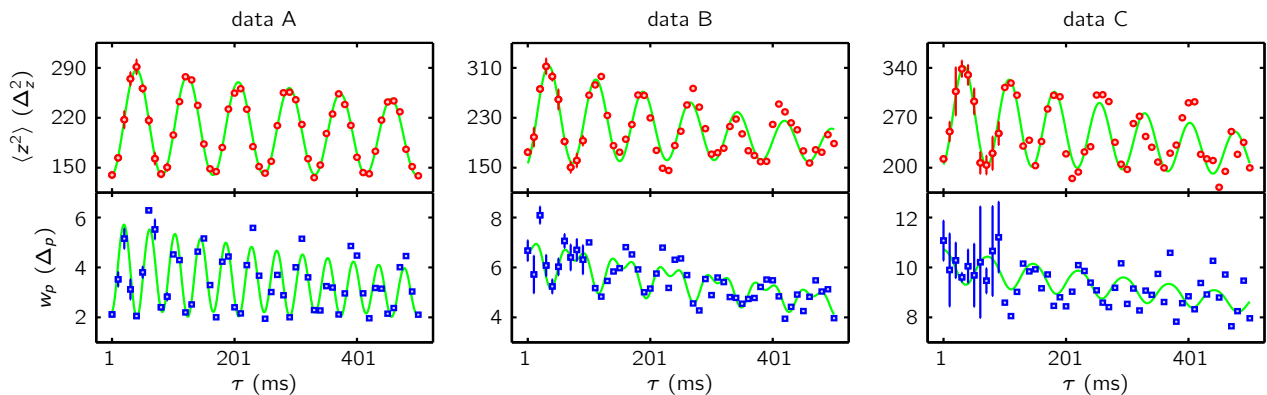


FIG. 2. Time evolution of the *in situ* mean-square width $\langle z^2 \rangle$ (top) and the momentum HWHM w_p (bottom) for 3 data sets. The solid lines show the fit: a damped sinusoid in real space (top), and a two-harmonic model according to Eq. (3) in momentum space (bottom). Statistical error of the widths are shown for the first 100 ms. Data A-C differ in thermodynamic regime. See Fig. 3 and text for details.

in excellent agreement with the inverted parabolas of the scaling solution. Self-similarity of the shapes is due to the fact the momentum distribution is dominated by the hydrodynamic velocity field, which is linear in position. The same phenomena is at the origine of the dynamic fermionization for a strongly interacting system [13].

Ideal Bose gas regime. For an IBG, a single-particle description suffices and breathing amounts to a rotation of the phase-space density, so that the widths in real and momentum space oscillate out of phase at the same frequency $\omega_B = 2\omega_D$. Fig. 2 shows a data set close to this regime (data C), where the *in situ* mean-square width $\langle z^2 \rangle$ (momentum HWHM w_p) is obtained from Gaussian (Lorentzian) fit. The antiphase is apparent from the plots. Fitting both time evolution with damped sinusoids, we measure identical breathing frequency, $\omega_B/\omega_D = 1.84 \pm 0.04$, where ω_D is determined by monitoring the center-of-mass (dipole) oscillations.

Crossover in real space. A central point to be understood is how the breathing frequency varies through the qBEC to IBG crossover. To address this question, we vary the total atom number in order to explore different regimes. The inset of Fig. 3 shows the region spanned by the data in the (γ, t) phase diagram of the LL model [28], where $\gamma = \frac{mg_{1D}}{\hbar^2 \rho}$ is the (local) interaction parameter, and $t = \frac{2\hbar^2 k_B T}{mg_{1D}^2}$ is the reduced temperature. Each sample is characterized by γ_0 , evaluated at the peak density. We extract $\langle z^2 \rangle$ from fitting $\rho(z)$ with either an inverted parabola for $\gamma_0 < 0.004$ [40] or a Gaussian otherwise. We obtain the real-space breathing frequency ω_{Bz} by fitting $\langle z^2 \rangle(\tau)$ with a damped sinusoid. The measured ω_{Bz}/ω_D as a function of γ_0 , shown in Fig. 3(a), displays a smooth crossover between the asymptotic theoretical limits $\sqrt{3}$ and 2 [11]. Such a frequency shift was first observed in [9], where the authors probed the breathing behaviour of an ensemble of 1D gases in real space. In addition to the issue of thermalization mentioned in [9], the intrinsic en-

semble averaging renders it problematic to characterize the system with a single value of temperature T or interaction parameter γ . In contrast, our current experiment with a single 1D system allows for a more quantitative study of the problem at hand.

In order to provide a theoretical treatment of the crossover, we devise two complementary approaches. On one hand, we model the crossover using the HDE Eq. (1). Since long-wavelength density waves in a fluid are adiabatic [41], we use the isentropic pressure curves derived numerically from the YY EoS [31]. The breathing mode frequency measured experimentally does not depend on the oscillation amplitude for the explored parameter range. We thus linearize the HDE for small displacement and ω_{Bz} is obtained by solving an eigenvalue problem. Results evaluated at $t = 1100$ are shown as a dashed line in Fig. 3(a). On the other hand, we provide a microscopic treatment of the breathing frequency that accounts for the effect of temperature. Assuming the system at $\tau = 0$ is at thermal equilibrium with a Hamiltonian $H = H_{LL} + H_{\text{pot}}$, $H_{\text{pot}} = m\omega_0^2 \sum_j z_j^2/2$, the expansion of the Heisenberg equation of motion after a quench $\Delta H = m(\omega_D^2 - \omega_0^2) \sum_j z_j^2/2$ gives $\langle \Delta H \rangle(\tau) = \langle \Delta H \rangle_T - \frac{\tau^2}{2} \langle C_2 \rangle_T + \frac{\tau^4}{4!} \langle C_4 \rangle_T + \dots$, where C_2 and C_4 are the second and fourth order nested commutators with $H_f = H + \Delta H$, and the thermal average $\langle \rangle_T$ is taken over the thermal state of H . Suppose the time evolution $\langle \Delta H \rangle(\tau) \propto \langle z^2 \rangle(\tau)$ is purely sinusoidal at the frequency ω_{Bz} , we have

$$\frac{\omega_{Bz}^2}{\omega_D^2} = \frac{\langle C_4 \rangle_T}{\langle C_2 \rangle_T} = 4 - \frac{1}{2} \frac{\langle H_{\text{int}} \rangle_T}{\langle H_{\text{pot}} \rangle_T}, \quad (2)$$

where $H_{\text{int}} = g_{1D} \sum_{j < k} \delta(z_j - z_k)$ is the interaction part of the Hamiltonian. The final equality comes from explicitly working out $\langle C_2 \rangle_T$ and $\langle C_4 \rangle_T$, and taking the limit of an infinitesimal quench amplitude $\alpha \rightarrow 1$, where the sinusoidal approximation is valid [42].

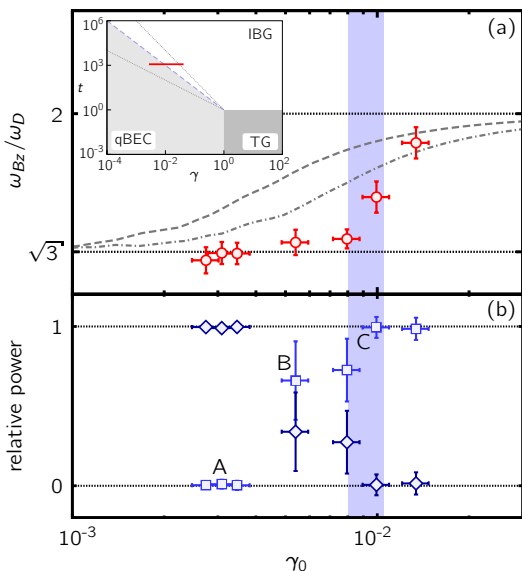


FIG. 3. Breathing mode through the crossover. (a) breathing frequency in units of dipole frequency, as a function of γ_0 . Our theory evaluated at $t = 1100$ (dashed line) and $t = 400$ (dash-dotted line) are shown. (b) relative power of the first (square) and second (diamond) harmonic of w_p . Data labels (A-C) correspond to those in Fig. 2. The errorbars account for fitting error only. The dotted lines are the asymptotic limits. The shaded region shows the crossover criteria $\gamma_{co} = t^{-2/3}$ (the dashed line in the inset), at $t \simeq 1100$ given by the *in situ* profile with 20% uncertainty. Inset: the phase diagram of the LL model [28], where all lines represent smooth crossovers. The horizontal line segment shows the region explored by the data [20].

It is remarkable that both approaches (HDE and the exact short-time expansion) give the same results for the breathing frequencies through the crossover. This indicates that the finite-temperature mass transport is indeed isentropic. Moreover, Eq. (2) extends the regime of validity of the existing sum-rule approaches, which erroneously predicts $\omega_{Bz} = \sqrt{2}\omega_D$ in IBG, whereas the true asymptotic limit is $\omega_{Bz} = 2\omega_D$.

Our theories provide a qualitatively good agreement with the experimental data, despite an overall overestimation of the breathing frequency. This quantitative departure most likely indicates that the atomic ensemble is not at thermal equilibrium at the end of the preparation (evaporation). Although the *in situ* profiles calibrated with the YY EoS generally yields about 100 nK, the atom-number fluctuation indicates approximately 35 to 45 nK at the center of the cloud. We thus include in Fig. 3(a) our prediction at $t = 400$ (dash-dotted line). We believe that such a lack of equilibrium is a direct consequence of evaporating into the integrable (1D) regime. Further investigation in this direction is underway.

Disappearance of the self-reflection mechanism. To address the behavior of the breathing mode in momentum space, we investigate the time evolution of w_p , ex-

tracted from a Lorentzian fit of $n(p)$. Since w_p shows a periodic behavior at the frequency ω_{Bz} , it can be expanded in a discrete Fourier spectrum. The relative weight of the Fourier components varies through the crossover, and we obtain quantitative information by fitting w_p with a function

$$y = Ae^{-\frac{\tau}{\tau_1}} + Be^{-\frac{\tau}{\tau_2}} \left[\sqrt{K} \cos(\omega_{Bz}\tau) - \sqrt{1-K} \cos(2\omega_{Bz}\tau) \right], \quad (3)$$

shown in Fig. 2 (bottom, solid line), with A fixed at the average width during the initial cycle and the phase corresponds to a minimal *in situ* width at the start of the oscillations. The relative power of the first harmonic K (squares) and second harmonic $1 - K$ (diamonds) are shown in Fig. 3(b) as a function of γ_0 . In qBEC, the second harmonic dominates, as predicted by the scaling solution, and signals the self-reflection mechanism. In IBG, the first harmonic dominates, as expected for a non-interacting gas where the self-reflection is absent. Both weights vary gradually through the crossover, indicating a smooth disappearance of the self-reflection mechanism. This can be seen as the effect the breathing mode has on the thermally excited Bogoliubov modes of high energy, e.g. their frequency and wavefunction would be modulated in time, such that w_p is larger at minimal $\langle z^2 \rangle$ than that at maximal $\langle z^2 \rangle$, see Fig. 2 (data B). The periodicity at $2\omega_{Bz}$ is then broken and the first harmonic at ω_{Bz} emerges. Figure 3 shows that the first harmonic starts to gain weight at a value of γ_0 significantly smaller than that where the frequency shift takes place in real space.

The breathing mode observed has lifetime estimated to be on the order of seconds. This is in stark contrast with situations in 3D where damping of the collective modes occurs, mainly via Landau damping mechanism [33, 34]. The long lifetime of the breathing mode in 1D may be related to the integrability of the underlying LL model.

Conclusions. In this Letter we have probed the breathing mode in real and momentum space through the qBEC to IBG crossover. The shift of the real-space frequency between the asymptotic values $\sqrt{3}\omega_D$ and $2\omega_D$ is demonstrated. Our theory models that assume thermal equilibrium before the quench do not agree with the measurement quantitatively, indicating the possibility of a non-Gibbs initial state produced by evaporation. We report the first observation of a momentum-space frequency doubling in qBEC, corresponding to an interaction-induced self-reflection mechanism that is expected of a Tonks gas. We experimentally map out the disappearance of the self-reflection through the crossover, for which no theoretical predictions exist to date. This illustrates the richness of out-of-equilibrium dynamics and the importance of the momentum-space observation to unveil the underlying physics.

The authors would like to thank A. Minguzzi, T. Roscilde, S. Stringari, P. Vignolo, M. Zvonarev for stimulating discussions. This work is financially supported by

Cnano IdF, the Austro-French FWR-ANR Project I607, and the FP7-Marie Curie IEF grant 327143.

-
- [1] S. Trotzky, Y.-A. Chen, A. Flesch, I. P. McCulloch, U. Schollwöck, J. Eisert, and I. Bloch, *Nat. Phys.* **8**, 325 (2012).
- [2] T. Langen, R. Geiger, M. Kuhnert, B. Rauer, and J. Schmiedmayer, *Nat. Phys.* **9**, 640 (2013).
- [3] M. Cheneau, P. Barmettler, D. Poletti, M. Endres, P. Schauß, T. Fukuhara, C. Gross, I. Bloch, C. Kollath, and S. Kuhr, *Nature* **481**, 484 (2012).
- [4] T. Kinoshita, T. Wenger, and D. S. Weiss, *Nature* **440**, 900 (2006).
- [5] M. Gring, M. Kuhnert, T. Langen, T. Kitagawa, B. Rauer, M. Schreitl, I. Mazets, D. A. Smith, E. Demler, and J. Schmiedmayer, *Science* **337**, 1318 (2012).
- [6] J. P. Ronzheimer, M. Schreiber, S. Braun, S. S. Hodgman, S. Langer, I. P. McCulloch, F. Heidrich-Meisner, I. Bloch, and U. Schneider, *Phys. Rev. Lett.* **110**, 205301 (2013).
- [7] A. Polkovnikov, K. Sengupta, A. Silva, and M. Vengalattore, *Rev. Mod. Phys.* **83**, 863 (2011).
- [8] M. A. Cazalilla, R. Citro, T. Giamarchi, E. Orignac, and M. Rigol, *Rev. Mod. Phys.* **83**, 1405 (2011).
- [9] H. Moritz, T. Stöferle, M. Köhl, and T. Esslinger, *Phys. Rev. Lett.* **91**, 250402 (2003).
- [10] E. Haller, M. Gustavsson, M. J. Mark, J. G. Danzl, R. Hart, G. Pupillo, and H.-C. Nägerl, *Science* **325**, 1224 (2009).
- [11] C. Menotti and S. Stringari, *Phys. Rev. A* **66**, 043610 (2002).
- [12] G. E. Astrakharchik, J. Boronat, J. Casulleras, and S. Giorgini, *Phys. Rev. Lett.* **95**, 190407 (2005).
- [13] A. Minguzzi and D. M. Gangardt, *Phys. Rev. Lett.* **94**, 240404 (2005).
- [14] M. Olshanii, *Phys. Rev. Lett.* **81**, 938 (1998).
- [15] A. H. van Amerongen, J. J. P. van Es, P. Wicke, K. V. Kheruntsyan, and N. J. van Druten, *Phys. Rev. Lett.* **100**, 090402 (2008).
- [16] J. Armijo, T. Jacqmin, K. V. Kheruntsyan, and I. Bouchoule, *Phys. Rev. Lett.* **105**, 230402 (2010).
- [17] T. Jacqmin, J. Armijo, T. Berrada, K. V. Kheruntsyan, and I. Bouchoule, *Phys. Rev. Lett.* **106**, 230405 (2011).
- [18] A. Vogler, R. Labouvie, F. Stubenrauch, G. Barontini, V. Guarrera, and H. Ott, *Phys. Rev. A* **88**, 031603 (2013).
- [19] J. Armijo, T. Jacqmin, K. Kheruntsyan, and I. Bouchoule, *Phys. Rev. A* **83**, 021605 (2011).
- [20] T. Jacqmin, B. Fang, T. Berrada, T. Roscilde, and I. Bouchoule, *Phys. Rev. A* **86**, 043626 (2012).
- [21] N. Fabbri, D. Clément, L. Fallani, C. Fort, and M. Inguscio, *Phys. Rev. A* **83**, 031604 (2011).
- [35] We remark that other thermometries are possible [19], and seem to indicate a lack of true equilibrium. See the discussions following Eq. (2) for more details.
- [23] Y. Castin and R. Dum, *Phys. Rev. Lett.* **77**, 5315 (1996).
- [36] Both the compression mode and the surface mode for an axially symmetric trap.
- [25] M. Girardeau, *J. Math. Phys.* **1**, 516 (1960).
- [37] We find a Gaussian point spread function of about 2 pixels in rms width sufficient to account for the broadening.
- [38] Assuming a system at thermal equilibrium in a trap $\omega_z = \omega_0$ and at the temperature obtained from independent calibration without the ω_z ramp.
- [28] K. V. Kheruntsyan, D. M. Gangardt, P. D. Drummond, and G. V. Shlyapnikov, *Phys. Rev. A* **71**, 053615 (2005).
- [39] The division is heuristically justified by the increasingly significant wings for greater values of γ_0 .
- [40] The two-fluid model that predicts a second sound in higher dimensions do not apply.
- [31] C. N. Yang and C. P. Yang, *J. Math. Phys.* **10**, 1115 (1969).
- [41] Eq. (2) could be used for a quench of finite amplitude ($\alpha \neq 1$) *a priori*. However, in the qBEC regime, a comparison with the scaling solution indicates that the sinusoidal approximation breaks down at finite α .
- [33] D. S. Jin, M. R. Matthews, J. R. Ensher, C. E. Wieman, and E. A. Cornell, *Phys. Rev. Lett.* **78**, 764 (1997).
- [34] P. O. Fedichev, G. V. Shlyapnikov, and J. T. M. Walraven, *Phys. Rev. Lett.* **80**, 2269 (1998).
- [35] Note1, we remark that other thermometries are possible [19], and seem to indicate a lack of true equilibrium. See the discussions following Eq. (2) for more details.
- [36] Note2, the validity of HDE for 1D Bose gases at finite temperature, for which a thermalisation time is unclear, is not established. Agreement with a different theoretical approach (see later in the text) strengthened this hypothesis.
- [37] Note3, both the compression mode and the surface mode for an axially symmetric trap.
- [38] Note4, we find a Gaussian point spread function of about 2 pixels in rms width sufficient to account for the broadening.
- [39] Note5, assuming a system at thermal equilibrium in a trap $\omega_z = \omega_0$ and at the temperature obtained from independent calibration without the ω_z ramp.
- [40] Note6, the division is heuristically justified by the increasingly significant wings for greater values of γ_0 .
- [41] Note7, the two-fluid model that predicts a second sound in higher dimensions do not apply.
- [42] Note8, eq. (2) could be used for a quench of finite amplitude ($\alpha \neq 1$) *a priori*. However, in the qBEC regime, a comparison with the scaling solution indicates that the sinusoidal approximation breaks down at finite α .